

Multi-resolution Spatial Regression for Aggregated Data with an Application to Crop Yield Prediction

Harrison Zhu* Adam Howes
Imperial College London
`{harrison.zhu15, adam.howes19}@imperial.ac.uk`

Owen van Eer, Maxime Rischard
Cervest
`{owen, maxime}@cervest.earth`

Dino Sejdinovic
University of Oxford
`dino.sejdinovic@stats.ox.ac.uk`

Seth Flaxman
Imperial College London
`s.flaxman@imperial.ac.uk`

May 27, 2022

Abstract

We develop a new methodology for spatial regression of aggregated outputs on multi-resolution covariates. Such problems often occur with spatial data, for example in crop yield prediction, where the output is spatially-aggregated over an area and the covariates may be observed at multiple resolutions. Building upon previous work on aggregated output regression, we propose a regression framework to synthesise the effects of the covariates at different resolutions on the output and provide uncertainty estimation. We show that, for a crop yield prediction problem, our approach is more scalable, via variational inference, than existing multi-resolution regression models. We also show that our framework yields good predictive performance, compared to existing multi-resolution crop yield models, whilst being able to provide estimation of the underlying spatial effects.

*Corresponding author.

1 Introduction

In spatial statistics, the widely-used technique of kriging is equivalent to what is known as Gaussian process (GP) regression (Rasmussen (2003)) in the machine learning community. This nonparametric technique has been successfully applied to crime (Flaxman et al. (2019)), air quality monitoring (Hamelijnck et al. (2019), remote sensing (Ton et al. (2018)) and epidemiology (Law et al. (2018a); Bhatt et al. (2017)). Although GP regression becomes computationally intractable for large datasets due to the $\mathcal{O}(n^3)$ and $\mathcal{O}(n^2)$ complexities of inverting and storing the kernel matrix, various approximation methods such as variational inference (Titsias (2009); Hensman et al. (2013, 2015a); Shi et al. (2020)) and the Integrated Nested Laplace Approximation (INLA) (Rue et al. (2016)) have been used to alleviate this.

We focus on performing inference in the case where the outputs are available at a lower spatial resolution than the covariates. Additionally, each of the covariates may have a different spatial resolution. For crop yield prediction, crop yields are only observed at the county level over an entire year due to the scarcity of agricultural census data (Burke et al. (2021)), whereas the covariates, such as satellite imagery, are abundantly available at daily temporal and pixel-level (e.g. 500m by 500m squares in space) spatial resolution. Similarly, in epidemiology, disease diagnostic data (Bhatt et al. (2017)) is also only available at the census (or aggregated) level due to privacy reasons. To accomplish prediction at the census level, a straightforward approach would be to spatially average the covariates within each census level in order to create a standard supervised learning dataset (Bhatt et al. (2017); Mateo-Sanchis et al. (2019)). The drawback of this approach is that it would result in a loss of within region-level variability and the ability for disaggregation modelling (Law et al. (2018a); Lucas et al. (2020)). For both problems of crop yield and epidemiology, high-resolution disaggregation can be very important for policy making as it would allow for interventions at a high precision. In this work we also present the first attempt, to the best of our knowledge, at disaggregation for crop yield modelling.

In the literature, this type of problem has recently been approached in many ways under the lens of regression with aggregated outputs (Gelfand (2010); Law et al. (2018a); Hamelijnck et al. (2019); Yousefi et al. (2019); Tanaka et al. (2019); Zhang et al. (2020)), distribution regression (Law et al. (2018b); Mateo-Sanchis et al. (2019); Adsuar et al. (2019); Lemercier et al. (2021)) and multiple instance learning (Maron and Lozano-Pérez (1998); Kim and De la Torre (2010)). Distribution regression has been widely used in the context of crop yield prediction (Thorns (2018); Mateo-Sanchis et al. (2019); Adsuar et al. (2019); Lemercier et al. (2021)) and the reason for this is partly because of its attractive theoretical properties (Szabó et al. (2016)) and ability to fuse together covariates at different resolutions (Thorns (2018); Adsuar et al. (2019)).

However, distribution regression is a computationally expensive procedure due to its $\mathcal{O}(\sum_{i,j=1}^n N_i N_j)$ complexity of computing the kernel matrix, where N_i and

N_j are the number of covariate vectors for outputs i and j . Typically, N_i and N_j may be of the order of 10^2 or 10^3 , depending on the resolution of the labels, and it will become computationally intractable to perform hyperparameter search. Previous methods that proposed to reduce this complexity include the use of random Fourier features (Rahimi and Recht (2008)), radial basis function (RBF) networks and Bayesian distribution regression (Law et al. (2018b)), at a slight cost to the approximation error.

Using the framework of aggregated output regression, where Gaussian process priors are often used for an underlying regression function, performing inference is still an expensive procedure. Exact inference or Markov chain Monte Carlo (MCMC) methods would still involve the $\mathcal{O}(\sum_{i,j=1}^n N_i N_j)$ complexity of computing the aggregated kernel matrix and would also prohibit hyperparameter tuning. Law et al. (2018a) and Yousefi et al. (2019) used variational inference to approximate the Gaussian process posterior, where one compresses all the information onto a set of M inducing points, and thereby bypassing the need for the full aggregated kernel matrix computation, reducing the computational complexity to $\mathcal{O}(M^3 + M^2 \sum_{i=1}^n N_i)$ and allowing for mini-batch training.

Contributions:

- We develop a new methodology of performing spatial regression with aggregated outputs and multi-resolution covariates by building upon VBAgg (Law et al. (2018a)). Our methodology could be interpreted as a generalisation of Law et al. (2018a) in the context of using satellite imagery covariates and is an extension of spatial kriging to the aggregated output setting due to the addition of an extra spatial effects component.
- We formulate a model, Multi-resolution Variational Bayes with Aggregated Output Gaussian Processes (MVBAgg), that extends Law et al. (2018a) by using multiple sets of inducing points for each resolution to perform variational inference. We thereby also inherit the attractive properties of computational tractability, ability for GPU-acceleration, uncertainty quantification and disaggregation of Law et al. (2018a). We then demonstrate that it gives good prediction performance relative to distribution regression, GPs trained on centroid covariates and VBAgg on a crop yield dataset located in the Corn Belt of the US (Adsuara et al. (2019); Mateo-Sanchis et al. (2019)).

2 Background

2.1 Distribution Regression:

Distribution regression is a method for nonparametric regression (Szabó et al. (2016)), which has been recently used for crop yield prediction (Thorns (2018); Mateo-Sanchis et al. (2019); Adsuara et al. (2019)). It assumes that the data

comes in the form of

$$\{(\Pi_i, y_i)\}_{i=1}^n,$$

where $y_i \in \mathbb{R}$ is a label, Π_i is a distribution over covariates $x \in \mathcal{X} \subseteq \mathbb{R}^d$, where $d \in \mathbb{N}_+$. In practice, Π_i is replaced with the empirical measure $\hat{\Pi}_i = N_i^{-1} \sum_{j=1}^{N_i} \delta_{x_{i,j}}$ for some observed covariates $\{x_{i,j}\}_{j=1}^{N_i}$, where $\delta_{x_{i,j}}$ is a Dirac measure centred at $\{x_{i,j}\}$ and $N_i \in \mathbb{N}_+$. Suppose that we want to find a predictive model \hat{f} that minimises the regularised empirical risk

$$\hat{f} := \operatorname{argmin}_{f \in \mathcal{H}_\rho} \frac{1}{n} \sum_{i=1}^n (y_i - f(\hat{\mu}_i))^2 + \lambda \|f\|_{\mathcal{H}_\rho}^2, \quad (1)$$

where $\hat{\mu}_i := \int_{\mathcal{X}} k(\cdot, x) d\hat{\Pi}_i(x) = N_i^{-1} \sum_{j=1}^{N_i} k(\cdot, x_{i,j})$ is the empirical mean embedding of $\hat{\Pi}_i$ into the reproducing kernel Hilbert space (RKHS) \mathcal{H}_k for some kernel $k : \mathcal{X} \times \mathcal{X} \rightarrow \mathbb{R}$. Solving (1) corresponds to *kernel ridge regression on the mean embeddings* (KRRe). Predictive functions f are taken from \mathcal{H}_ρ , the RKHS of a second-level kernel $\rho : \mathcal{H}_k \times \mathcal{H}_k \rightarrow \mathbb{R}$, and λ is a regularisation parameter. Given any set of covariates $\{x_{*,j}\}_{j=1}^{N_*}$, where $N_* \in \mathbb{N}_+$, and using the kernel trick, this yields a solution $\hat{f}(\hat{\mu}_*) = K_* \tilde{\alpha}$, for $\hat{\mu}_* = N_*^{-1} \sum_{j=1}^{N_*} k(\cdot, x_{*,j})$, where

$$\begin{aligned} K_* &:= (\rho(\hat{\mu}_*, \hat{\mu}_1), \dots, \rho(\hat{\mu}_*, \hat{\mu}_n)), \\ \tilde{\alpha} &:= (K + \lambda I_n)^{-1} y, \end{aligned}$$

with $(K)_{i,j} = \rho(\hat{\mu}_i, \hat{\mu}_j)$. Using the kernel trick again and with the linear kernel $\rho(f, g) = \langle f, g \rangle_{\mathcal{H}_k}$, this recovers *linear regression on the mean embeddings* (LRe), in which $(K)_{i,j} = (N_i N_j)^{-1} \sum_{l=1}^{N_i} \sum_{r=1}^{N_j} k(x_{i,l}, x_{j,r})$ and I_n being the n -dimensional identity matrix. Note that the LRe also employs the *kernel trick* since mean embeddings are potentially infinite-dimensional, i.e. no explicit coefficients of the linear model are used. Similarly, one can also use a non-linear kernel ρ , which we call *kernel ridge regression on the mean embeddings* (KRRe), and this has been shown to improve its performance in certain scenarios (Muandet et al. (2012)).

A major disadvantage of distribution regression is the need to perform $\mathcal{O}(\sum_{i=1}^n \sum_{j=1}^n N_i N_j)$ number operations to compute the matrix K , and a subsequent $\mathcal{O}(n^3)$ to invert $K + \sigma^2 I_n$, therefore prohibiting the ability to efficiently tune the regularisation parameter λ and kernel hyperparameters of k (in contrast to the hyperparameters of ρ , which can be tuned more efficiently). It is also possible to make use of RBF networks and Bayesian distribution regression (Law et al. (2018b)) by inducing points approximations, and RFF to approximate the kernel matrix (Rahimi and Recht (2008)) for improving the computational scalability.

2.2 Gaussian Process for Aggregated Output Regression

GPs can be used to tackle *aggregated output regression* (Law et al. (2018a); Hamelijnck et al. (2019); Tanaka et al. (2019); Yousefi et al. (2019)). This is a

common setting in spatial statistics, where each label is often associated with a set of observations within a region (areal unit). Again, suppose we have some covariate space \mathcal{X} and a response space \mathbb{R} . The aggregated output regression model (Tanaka et al. (2019)) is defined as

$$y_i = \int_{\mathcal{X}_i} f(x) d\Pi_i(x) + \epsilon_i, \quad \epsilon_i \sim \mathcal{N}(0, \sigma^2), \quad (2)$$

where $\mathcal{X}_i \subseteq \mathcal{X}$ is an observation region with distribution Π_i with Lebesgue density π_i and ϵ_i is an independently distributed Gaussian noise with $\sigma > 0$. We denote $\mathcal{N}(a, b)$ and $N(\cdot; a, b)$ as the distribution and density function of a Gaussian distribution with mean a and covariance b .

In practice, we will want to approximate $\int_{\mathcal{X}_i} f(x) d\Pi_i(x)$ using some available covariates $\{x_{i,j}\}_{j=1}^{N_i}$ drawn from Π_i . In general, this integral could be approximated by constructing quadrature weights $w_{i,j}$ and states $\{x_{i,j}\}_{j=1}^{N_i}$ and integrating with respect to $\hat{\Pi}_i = \sum_{j=1}^{N_i} w_{i,j} \delta_{x_{i,j}}$ such that $\sum_{j=1}^{N_i} w_{i,j} = 1$. Law et al. (2018a) used deterministic survey weights and Hamelinck et al. (2019) constructed the weights using a Gaussian process regression network, but it is not clear how these will improve the estimation accuracy of $\int_{\mathcal{X}_i} f(x) d\Pi_i(x)$ and so we will assume that $w_{i,j} = N_i^{-1}$ for all $j = 1, \dots, N_i$. In the context of classification of images, alternative aggregation methods are max-aggregation or attention-aggregation (Kim and De la Torre (2010); Haussmann et al. (2017); Ilse et al. (2018)).

Using this setup, we thus work with the dataset

$$\{(\{x_{i,j}, w_{i,j}\}_{j=1}^{N_i}, y_i)\}_{i=1}^n.$$

Using $\hat{\Pi}_i$, Equation 2 becomes

$$y_i = \sum_{j=1}^{N_i} w_{i,j} f(x_{i,j}) + \epsilon_i, \quad \epsilon_i \sim \mathcal{N}(0, \sigma^2), \quad (3)$$

where f is some underlying regression function and $\sigma > 0$. We can posit a GP prior $f \sim \mathcal{GP}(m, k)$, where m and k are the mean and covariance functions, in order to infer f . We will denote the likelihood function of (3) as $p(y_i|f_i)$, where $f_i := (f(x_{i,1}), \dots, f(x_{i,N_i}))^\top$, and denote the weights $w_i := (w_{i,1}, \dots, w_{i,N_i})^\top$. Similarly, denote $f_* := (f_{*,1}, \dots, f_{*,N_*})^\top$ for prediction points $\{x_{*,j}, w_{*,j}\}_{j=1}^{N_*}$ with true label y_* . Suppose further that $X_i := (x_{i,1}, \dots, x_{i,N_i})^\top$, $X_* := (x_{*,1}, \dots, x_{*,N_*})^\top$ and $k_{X_i, X_j} := (k(x_{i,l}, x_{j,m}))_{l,m}$ for pairs i, j , and $l = 1, \dots, N_i$ and $m = 1, \dots, N_j$,

The log-likelihood is $\log p(y_i|f_i)$ is

$$\log p(y_i|f_i) = -\frac{1}{2\sigma^2} (y_i - w_i^\top f_i)^2 - \frac{1}{2} \log (2\pi\sigma^2).$$

Since we have

$$\begin{pmatrix} y_1 \\ \vdots \\ y_n \\ w_*^\top f_* \end{pmatrix} = \mathcal{N} \left(\begin{pmatrix} w_1^\top m_{X_1} \\ \vdots \\ w_n^\top m_{X_n} \\ w_*^\top m_{X_*} \end{pmatrix}, \begin{pmatrix} K + \sigma^2 I_n & K_* \\ K_*^\top & K_{*,*} \end{pmatrix} \right),$$

where $(K)_{ij} = (w_i^\top k_{X_i, X_j} w_j)_{ij}$, $(K_*)_i := (w_i^\top k_{X_i, X_*} w_*)_i$ and $K_{*,*} := w_*^\top k_{X_*, X_*} w_*$, by standard identities of Gaussian distributions we have the conditional distribution

$$w_*^\top f_* | \{(\{x_{i,j}, w_{i,j}\}_{j=1}^{M_i}, y_i)\}_{i=1}^n \sim \mathcal{N}(\tilde{m}_{X_*}, \tilde{k}_{X_*, X_*}),$$

with

$$\begin{aligned}\tilde{m}_{X_*} &:= w_*^\top m_{X_*} + K_*^\top (K + \sigma^2 I_n)^{-1} (y - m_X), \\ \tilde{k}_{X_*, X_*} &:= K_{*,*} - K_*^\top (K + \sigma^2 I_n)^{-1} K_*.\end{aligned}$$

With a zero mean function, the posterior mean obtained here is the exact expression from LRe, similar to the connection between standard, non-aggregated GP regression and kernel ridge regression (Kanagawa et al. (2018)). With this, we are still prohibited by the large computational burden in the kernel matrix operations.

On the other hand, if Π_i is known, then we would obtain

$$\begin{pmatrix} y_1 \\ \vdots \\ y_n \\ \int_{\mathcal{X}_*} f_*(u) \pi_*(x) dx \end{pmatrix} = \mathcal{N} \left(\begin{pmatrix} \int_{\mathcal{X}_1} m(x) \pi_1(x) dx \\ \vdots \\ \int_{\mathcal{X}_n} m(x) \pi_n(x) dx \\ \int_{\mathcal{X}_*} m(x) \pi_*(x) dx \end{pmatrix}, \begin{pmatrix} K + \sigma^2 I_n & K_* \\ K_*^\top & K_{*,*} \end{pmatrix} \right),$$

where

$$\begin{aligned}(K)_{ij} &:= \int_{\mathcal{X}_i} \int_{\mathcal{X}_j} k(u, v) \pi_i(u) \pi_j(v) du dv, \\ (K_*)_i &:= \int_{\mathcal{X}_*} \int_{\mathcal{X}_i} k(u, v) \pi_*(u) \pi_i(v) du dv, \\ K_{*,*} &:= \int_{\mathcal{X}_*} \int_{\mathcal{X}_*} k(u, v) \pi_*(u) \pi_*(v) du dv.\end{aligned}$$

The posterior distribution over the integral $\int_{\mathcal{X}_*} f(x) d\Pi_*(x)$ would thus be

$$\int_{\mathcal{X}_*} f(x) d\Pi_*(x) \sim \mathcal{N}(\tilde{m}, \tilde{k}),$$

with

$$\begin{aligned}\tilde{m} &:= \int_{\mathcal{X}_*} m(x) \pi_*(x) dx + K_*^\top (K + \sigma^2 I_n)^{-1} (y - m_X), \\ \tilde{k} &:= K_{*,*} - K_*^\top (K + \sigma^2 I_n)^{-1} K_*.\end{aligned}$$

Having learned the posterior distribution of f , it is then possible to make predictions and provide statistical insights at the individual covariate level (Law et al. (2018a)).

2.3 Variational Bayes with Gaussian Processes (VBAgg)

Although kernel ridge and exact Gaussian process regression provide elegant inference procedures for learning from aggregated outputs, the computational

complexity prohibits the ability to tune hyperparameters in a data-driven way. Following Law et al. (2018a) and Yousefi et al. (2019), which use the Sparse Variational GP (SVGP) framework of Titsias (2009); Hensman et al. (2013) and Hensman et al. (2015a), we will use a set of M inducing points $u = (f(z_1), \dots, f(z_M))^\top$ at locations $Z = (z_1, \dots, z_M)^\top$, with $z_1, \dots, z_M \in \mathbb{R}^d$. We pose a variational distribution $q(f, u) := p(f|u)q(u)$ and minimise $\text{KL}(q(f, u)||p(f, u|y))$ to give the variational approximation

$$q(u) = \text{argmin}_{q \in \mathcal{Q}} \text{KL}(q(u)||p(u)) - \sum_{i=1}^n \int \log\{p(y_i|f_i)\}q(u)p(f_i|u) \, du \, df_i,$$

that is close to the true posterior $p(f, u|y)$. We choose the variational family $\mathcal{Q} = \{q(u) = N(u; \eta_Z, \Sigma_Z) : \eta_Z \in \mathbb{R}^M, \Sigma_Z \in \mathbb{R}^{M \times M}\}$. Since $p(f_i|u) = N(\hat{m}_{X_i}, \hat{k}_{X_i, X_i})$ with

$$\begin{aligned} \hat{m}_{X_i} &= m_{X_i} + k_{X_i, Z} k_{Z, Z}^{-1} (u - m_Z), \\ \hat{k}_{X_i, X_i} &= k_{X_i, X_i} - k_{X_i, Z} k_{Z, Z}^{-1} k_{Z, X_i}, \end{aligned}$$

the approximate posterior is thus $q(f_i) := \int p(f_i|u)q(u)du = N(f_i; \tilde{m}_{X_i}, \tilde{k}_{X_i, X_i})$ where

$$\begin{aligned} \tilde{m}_{X_i} &= m_{X_i} + k_{X_i, Z} k_{Z, Z}^{-1} (\eta_Z - m_Z), \\ \tilde{k}_{X_i, X_i} &= k_{X_i, X_i} - k_{X_i, Z} (k_{Z, Z}^{-1} - k_{Z, Z}^{-1} \Sigma_Z k_{Z, Z}^{-1}) k_{Z, X_i}. \end{aligned}$$

This thus allows the lower bound to be written down explicitly as

$$\mathcal{L} := \text{KL}(q(u)||p(u)) - \frac{1}{2} \sum_{i=1}^n \left(\frac{y_i^2 - 2y_i w_i^\top \tilde{m}_{X_i} + w_i^\top (\tilde{k}_{X_i, X_i} + \tilde{m}_{X_i} \tilde{m}_{X_i}^\top) w_i}{\sigma^2} - \log(2\pi\sigma^2) \right),$$

and solved via optimisation methods in mini-batches (via a stochastic approximation to \mathcal{L} . See Zhang et al. (2019) for a review). One could also sample the optimal posterior distribution, in which $\text{KL}(q(f, u)||p(f, u|y)) = 0$, directly using MCMC, as proposed in Hensman et al. (2015b). To make a prediction for an arbitrary region with N_* inputs X_* , this simply requires the posterior distribution

$$q(w_*^\top f_*) = N(w_*^\top f_*; w_*^\top \tilde{m}_{X_*}, w_*^\top \tilde{k}_{X_*, X_*} w_*).$$

3 Aggregated Output Spatial Regression

In spatial statistics, we often make use of spatially-resolved covariates, where we implicitly assume that they are a function of the spatial coordinates. Suppose that $\mathcal{S} \subseteq \mathbb{R}^2$ represents a spatial domain and $g : \mathcal{S} \rightarrow \mathbb{R}^d$, where $d > 0$, is an unknown function that represents a covariate. Then g , for example, could be the solution of the heat equation if it represents temperature, although in reality we may only observe a noisy version of g collected via remote sensing methods,

such as satellite sensors and cameras. We can thus formulate aggregated output spatial regression as

$$y_i = \frac{1}{|\mathcal{S}_i|} \int_{\mathcal{S}_i} f^1(g(s))ds + \frac{1}{|\mathcal{S}_i|} \int_{\mathcal{S}_i} f^0(s)ds + \epsilon_i, \quad \epsilon_i \sim \mathcal{N}(0, \sigma^2), \quad (4)$$

where $\mathcal{S}_i \subseteq \mathcal{S}$, and f^1 and f^2 are functions indicating effects from remote sensing covariates and additional spatial variability. Note that the first integral can also be written as $\frac{1}{|\mathcal{S}_i|} \int_{\mathcal{T}_i} f^1(t)d(g_{\sharp}\lambda)(t)$, where λ is the Lebesgue measure, $g_{\sharp}\lambda$ is the push-forward measure and $g^{-1}(\mathcal{T}_i) = \mathcal{S}_i$, meaning that we can use the aggregated output models as previously discussed. It is interesting to note that λ could also be other measures, such as the spherical measure, a generalisation of the Lebesgue measure on the sphere $\mathbb{S}^2 \subset \mathbb{R}^3$ and may be a more realistic measure for modelling Earth observations.

In the context of images, such as ones obtained via satellites, each datapoint represents a pixel, which is a square over space, as shown in Figure 1. It should be noted that this limits the number of points that one can use for performing numerical integration as it would depend on the spatial resolution of the covariates. For each pixel, suppose we have a representative latitude-longitude pair $[s]$. For a subset with latitude and longitude $\mathcal{S} \subseteq \mathbb{R}^2$ and Lebesgue measure λ , this means that we have to discretise the domains \mathcal{S}_i into a discrete measure space $\widehat{\mathcal{S}}_i$ of the representatives $[s]$, with measure $\widehat{\lambda}_i(S) = \frac{1}{|\widehat{\mathcal{S}}_i|} \sum_{s \in S} \mathbb{1}_{\widehat{\mathcal{S}}_i}(s)$ for any $S \subseteq \widehat{\mathcal{S}}_i$. This changes Equation 4 to

$$y_i = \frac{1}{|\widehat{\mathcal{S}}_i|} \sum_{s \in \widehat{\mathcal{S}}_i} f^1(g(s)) + \frac{1}{|\mathcal{S}_i|} \int_{\mathcal{S}_i} f^0(s)ds + \epsilon_i, \quad \epsilon_i \sim \mathcal{N}(0, \sigma^2), \quad (5)$$

where we note that we can still approximate the second integral with *arbitrarily many* points in space without discretisation as the spatial covariates have infinite resolution. In contrast, Law et al. (2018a) only allows for a single integral and the number of spatial points must match the number of pixels for the spatially-resolved covariates.

As it is the case that the covariate effects from $g(s)$ and spatial effects from s do not need to be treated at the same resolution, various spatially-resolved covariates may also correspond to different resolutions. In previous aggregated output modelling works, the covariates are usually preprocessed to the same resolution (Mateo-Sanchis et al. (2019)). This means that when using aggregate output methods, the integrals of the mean and covariance functions will be integrated over a discrete measure with fewer points, giving less accurate and higher variance approximations. On the other hand, up-sampling may result in errors from the approximation algorithms used, introducing bias into the integrals. This thus motivates the use of multi-resolution models, where the integrals for different resolution are separated without up-sampling or down-sampling by assuming an additive structure. Suppose we have D covariates, each with a different spatial resolution. By treating each resolution separately, we can modify Equation 5 and obtain

$$y_i = \sum_{l=1}^D \frac{1}{|\widehat{\mathcal{S}}_{i,l}|} \sum_{s \in \widehat{\mathcal{S}}_{i,l}} f^k(g_l(s)) + \frac{1}{|\mathcal{S}_i|} \int_{\mathcal{S}_i} f^0(s)ds + \epsilon_i, \quad \epsilon_i \sim \mathcal{N}(0, \sigma^2),$$

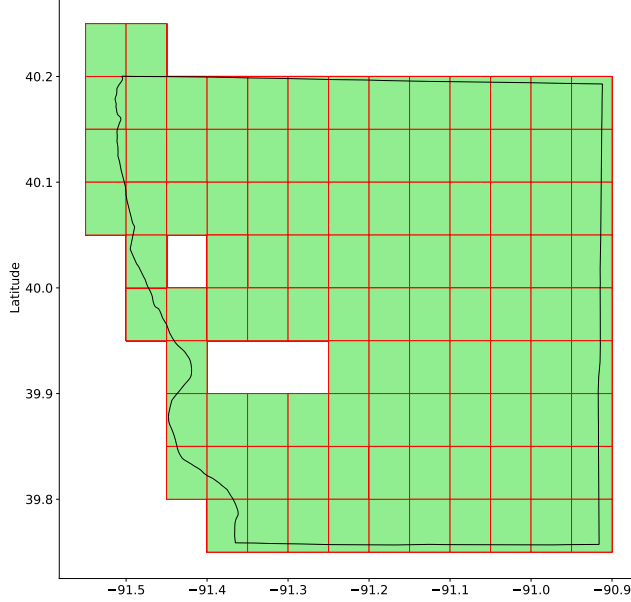


Figure 1: Pixel squares of the MCD12C1 land cover mask (Friedl and Sulla-Menashe (2015)) over Adams county, Illinois, USA. Note that some of the data is missing, as represented by the white squares.

for resolutions $l = 1, \dots, D$ and $g_l : \mathcal{S} \rightarrow \mathbb{R}^{d_l}$ for $d_l > 0$. Note that we here consider an additive model across covariates corresponding to different resolutions. This results in the additive covariance kernel structure. It is also possible to formulate a product covariance kernel structure, but we do not pursue it further in this work.

3.1 Multi-resolution Variational Bayes with Aggregated Output Gaussian Processes (MVBAgg)

A natural extension to VBAgg is to include covariates of multiple sets and hence observing the dataset

$$\{(\{\{x_{i,j,l}, w_{i,j,l}\}_{j=1}^{N_{i,l}}\}_{l=1}^D, y_i)\}_{i=1}^n,$$

where $l = 1, \dots, D$ is the index of the covariates. Adsuara et al. (2019) proposes incorporating sets of covariates at different resolutions, in the context of LRe, by considering kernel regression functions in the space equal to the direct sum of RKHSs with kernels ρ_1, \dots, ρ_D , where $\rho_l : \mathcal{H}_{k_l} \times \mathcal{H}_{k_l} \rightarrow \mathbb{R}$. From a GP point of view, we may learn similar functions by modifying Equation 3 to

$$y_i | \{\{x_{i,j,l}, w_{i,j,l}\}_{j=1}^{N_{i,l}}\}_{l=1}^D \sim \mathcal{N} \left(\sum_{l=1}^D \sum_{j=1}^{N_{i,l}} w_{i,j,l} f^l(x_{i,j,l}), \left(\sum_{l=1}^D \sum_{j=1}^{N_{i,l}} w_{i,j,l}^2 \right) \sigma^2 \right),$$

where f^l is a function induced with a GP prior $\mathcal{GP}(0, k_l)$ with kernel $k_l : \mathcal{X}_{i,l} \times \mathcal{X}_{i,l} \rightarrow \mathbb{R}$, where $\mathcal{X}_{i,l}$ is the covariate space for the l th resolution in the region indexed by i . We assume that the f^l 's are mutually independent. To use a VBAgg approximation framework, we pose the variational distribution $q(f^1, \dots, f^D, u_1, \dots, u_D) := \prod_{l=1}^D p(f^l|u_l)q(u_l)$ with different inducing points $u_l = (f^l(z_{1,l}), \dots, f^l(z_{L_l,l}))^\top$ at each sets of locations $Z_l = (z_{1,l}, \dots, z_{L_l,l})^\top$. We can thus obtain the approximate posterior $q(f^l)$ for each l as $q(f_i^l) = N(f_i^l; \tilde{m}_{X_{i,l}}, \tilde{k}_{X_{i,l}, X_{i,l}})$

$$\begin{aligned}\tilde{m}_{X_{i,l}} &= m_{X_{i,l}} + k_{X_{i,l}, Z_l} k_{Z_l, Z_l}^{-1} (\eta_{Z_l} - m_{Z_l}), \\ \tilde{k}_{X_{i,l}, X_{i,l}} &= k_{X_{i,l}, X_{i,l}} - k_{X_{i,l}, Z_l} (k_{Z_l, Z_l}^{-1} - k_{Z_l, Z_l}^{-1} \Sigma_{Z_l} k_{Z_l, Z_l}^{-1}) k_{Z_l, X_{i,l}},\end{aligned}$$

where $X_{i,l} := (x_{i,1,l}, \dots, x_{i,N_{i,l},l})^\top$. The lower bound can then be written as

$$\begin{aligned}\mathcal{L} &:= \sum_{l=1}^D \text{KL}(q(u_l) || p(u_l)) \\ &\quad - \frac{1}{2} \sum_{i=1}^n \left(\frac{1}{\sigma^2} [y_i^2 - 2y_i \sum_{l=1}^D w_{i,l}^\top \tilde{m}_{X_{i,l}} + \sum_{l=1}^D w_{i,l}^\top (\tilde{k}_{X_{i,l}, X_{i,l}} + \tilde{m}_{X_{i,l}} \tilde{m}_{X_{i,l}}^\top) w_{i,l}] \right. \\ &\quad \left. - \log(2\pi\sigma^2) \right),\end{aligned}$$

where $w_{i,l} := (w_{i,1,l}, \dots, w_{i,N_{i,l},l})^\top$. Similarly, the predictive distribution for y_* would be

$$q(\sum_{l=1}^D w_{*,l}^\top f_*^l) = N(\sum_{l=1}^D w_{*,l}^\top f_*^l; \sum_{l=1}^D w_{*,l}^\top \tilde{m}_{X_{*,l}}, \sum_{l=1}^D w_{*,l}^\top \tilde{k}_{X_{*,l}, X_{*,l}} w_{*,l}).$$

To initialise the inducing points Z_k 's, we follow the setup in VBAgg (Law et al. (2018a)) and pick 1 point from each region i using the cluster centres with KMeans. We can also set the inducing points to be trainable or fixed. Inheriting the nice properties of VBAgg, we can attain $\mathcal{O}(\sum_{l=1}^D L_l^3 + L_l^2 \sum_{i=1}^n N_{i,l})$ complexity in time, can performing mini-batch training and make use of GPU-acceleration. In comparison, Adsuara et al. (2019) gives $\mathcal{O}(\sum_{l=1}^D \sum_{i,j=1}^n N_{i,l} N_{j,l})$ complexity. Although it is possible to employ RFF to give a reduction to $\mathcal{O}(\sum_{l=1}^D L_l^3 + L_l^2 \sum_{i=1}^n N_{i,l})$, where L_l is now the dimension of the RFF map, it still cannot perform kernel parameter tuning without cross-validation, whereas we propose to tune the parameters in a data-driven way via the variational lower bound. The full inference scheme is detailed in Algorithm 1.

Returning to the context of aggregated outputs in the spatial context, alongside sets of remote sensing covariates, we would also include a set of latitude and longitude coordinates that we can sample uniformly on the continuous spatial domain. This yields the spatial GP f^0 and the covariate GPs f^1, \dots, f^D . As motivated in Law et al. (2018a), the VBAgg model is also capable of performing disaggregation by learning an analytic form of the approximate posterior distribution on the underlying function f . In a similar manner, with MVBAgg we can also study each of the GPs at the pixel level using the posterior distribution of each f^l .

Algorithm 1 Training of Multi-resolution Variational Bayes with Aggregated Output Gaussian Processes (MVBAgg)

Input $\{\{x_{i,j,l}, w_{i,j,l}\}_{j=1}^{N_{i,l}}, y_i\}_{i=1}^n$ (dataset), $\{z_l\}_{l=1}^D$ (landmark points), $\{\eta_{Z_l}\}_{l=1}^D$, $\{\Sigma_{Z_l}\}_{l=1}^D$ (variational distribution parameters), kernels $\{k_l\}_{l=1}^D$, noise σ , total iterations L , batch size B

- 1: Initialise ELBO $\mathcal{L} \leftarrow 0$
- 2: **for** $i = 1, \dots, L$ **do**
- 3: Take a mini-batch $\{\{x_{i,j,l}, w_{i,j,l}\}_{j=1}^{N_{i,l}}, y_i\}_{i \in B}$ with indexing set $B \subset \{1, \dots, n\}$
- 4: Compute lower bound \mathcal{L}_B with this batch
- 5: $\mathcal{L} \leftarrow \mathcal{L} + \frac{n}{B} \mathcal{L}_B$
- 6: **if** $i \bmod n/B = 0$ **then**
- 7: Backpropagate \mathcal{L} and update model parameters
- 8: **end if**
- 9: **end for**
- 10: **return** $\{k_l\}_{l=1}^D, \sigma, \{\eta_{Z_l}\}_{l=1}^D, \{\Sigma_{Z_l}\}_{l=1}^D$

4 Application to Crop Yield prediction

The task of crop yield prediction has recently been attempted by scientists using a variety of methods (Bolton and Friedl (2013); Kuwata and Shibasaki (2015); Lobell et al. (2015); You et al. (2017); Thorns (2018); Mateo-Sanchis et al. (2019); Adsuara et al. (2019); Yang et al. (2019); Lemercier et al. (2021)). The wide availability of remote sensing and geophysical data from NASA programmes such as Moderate Resolution Imaging Spectroradiometer (MODIS) (Didan (2015)) and Soil Moisture Active Passive (SMAP) (Entekhabi et al. (2010)) have also helped with this effort by providing modellers with pixel-resolution information on croplands. By utilising the vast amount of data, such as vegetation indices, that have biological links to crop health and hence to yield (Mateo-Sanchis et al. (2019)), as covariates of the croplands, modellers can formulate crop yield prediction as a supervised learning problem. However, existing works on crop yield modelling using aggregated output/distribution regression methods (You et al. (2017); Thorns (2018); Mateo-Sanchis et al. (2019); Adsuara et al. (2019)) do not consider the model uncertainty and interpretability, which is arguably as important as performing crop yield prediction itself.

Our work is most closely related to kernel methods for crop yield modelling, notably multi-source kernel ridge regression (on the mean embeddings) (Adsuara et al. (2019)), kernel ridge regression (Mateo-Sanchis et al. (2019)) and Bayesian distribution regression (Thorns (2018)). Another very popular approach is to extract signals from the image histograms of the pixel values using convolutional neural networks, as attempted in the Deep Gaussian process for crop yield prediction work (You et al. (2017)). However, this approach is not suitable for accounting for the underlying spatial structure and variability due to the the use

of image histograms, whereas our method keeps the pixel-level spatial structure. Our aim is to both predict the crop yield at the county-level and disaggregate the underlying spatial random surface at the pixel-level

4.1 Data

We use a county-level crop yield dataset from Mateo-Sanchis et al. (2019) with yield in the U.S. Corn Belt in 2015, vegetation optical depth (VOD) (Konings et al. (2017)) derived from the SMAP products (Entekhabi et al. (2010)) and Enhanced Vegetation Index (EVI) from MODIS (Didan (2015)). Unfortunately, the covariates in this study are in the same spatial resolution due to the downsampling of the EVI covariates and the data processing procedure is non-trivial, but we can nonetheless obtain a multi-resolution dataset by adding sets of 100 spatial covariates (latitude + longitude in EPSG:4326 projection format) per county. Following Sanchis et al. (2019), we use only use covariates during the period April 2015 - October 2015, which covers the period from growth to just before harvest. For VOD and EVI respectively, this gives 213 and 13 observations for each spatial location respectively. We filter out regions where the geometry of the yield has not been provided, giving 375 outputs as shown in Figure 2.

4.2 Experimental Setup

For our experiments, we will assess the performance of the predictive models via 5-fold cross-validation, reporting the Root Mean Squared Error (RMSE) $\sqrt{\frac{1}{n} \sum_{i=1}^n (y_i - \hat{y}_i)^2}$ and Mean Average Percentage Error (MAPE) $\frac{1}{n} \sum_{i=1}^n |(y_i - \hat{y}_i)/y_i|$, averaged over 5 validation sets, with 300 and 75 training and test labels respectively per fold. Our benchmarks are Linear Regression (LR), Gaussian process (GP) regression, linear regression on the mean embeddings (LRe), kernel ridge regression on the mean embeddings (KRRe) and VBAgg. We compare these to MVBAgg. For LR and GP, we use the centroid covariates, where we spatially average the covariates to obtain a standard supervised learning dataset. For all other models, we use the “stacked covariates” (Thorns (2018); Mateo-Sanchis et al. (2019); Adsuara et al. (2019)), where each column represents an observation at a certain time during the year and each row presents an observation at a certain spatial location. For MVBAgg, VBAgg and GP, the VOD and EVI covariates are treated in the same resolution with additive RBF kernels, defined as:

$$k(x, y) = \sigma^2 \exp\left(-\frac{\|x-y\|_2^2}{2\ell^2}\right), \quad \forall x, y \in \mathcal{X},$$

where $\sigma > 0$ is the scale, $\ell > 0$ is the lengthscale and $\|\cdot\|_2$ denotes the Euclidean norm. Similarly, the spatial components are specified with a Matérn-3/2 kernel:

$$k(x, y) = \sigma^2 \left(1 + \frac{\sqrt{3}\|x-y\|_2}{\ell}\right) \exp\left(-\frac{\sqrt{3}\|x-y\|_2}{\ell}\right).$$

We fit LR and GP using maximum likelihood estimation, and LRe and KRRe using the median heuristic for the lengthscale¹ (Garreau et al. (2018)) and the scale $\sigma = 1$, with a regularisation parameter of $\lambda = 0.1$. In addition, LRe and KRRe use the linear and RBF second-level kernel respectively, in which for the latter we tune the lengthscale also using the median heuristic (of the difference of the mean embedding norms $\|\hat{\mu}_i - \hat{\mu}_j\|_{\mathcal{H}_\rho}$ for counties i, j) and set $\sigma = 1$. We use the Adam optimiser with a learning rate of 0.001, 20,000 training iterations and the inducing points chosen by taking the centre of a K-Means algorithm (Oglic and Gärtner (2017)) in each county for MVBAgg and VBAgg. We relied on GPFlow (De G. Matthews et al. (2017)) and NumPy (Harris et al. (2020)) to implement our models. The code is available at <https://github.com/ImperialCollegeLondon/MVBAgg>. For VBAgg and MVBAgg, we used 2 Nvidia RTX 2080 GPUs, and for all the other methods, we used Intel(R) Xeon(R) Gold 6242 CPU @ 2.80GHz CPUs, both on the NVIDIA4 GPU Compute Server provided by the Department of Mathematics, Imperial College London.

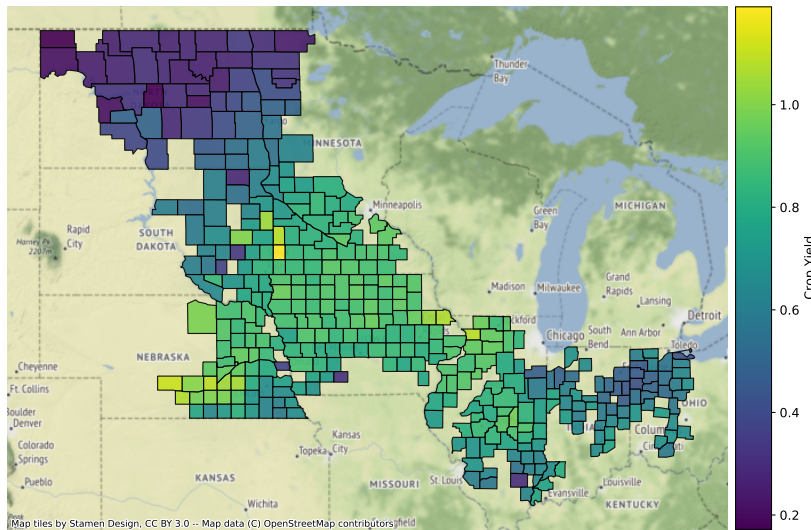


Figure 2: Crop yield (kg/m^2) in the corn belt of the United States.

4.3 Results

We can see from Table 1 that the out-of-sample predictive performance for MVBAgg is slightly better than GP, LRe and KRRe in terms of RMSE and MAPE. Due to the larger difference in MAPE, we can interpret this as MVBAgg giving better individual county predictions on average. In many applications,

¹As there are over 20,000 covariate values, we take a maximum of 10 values per county, which reduces this number to around 3,000, and then compute the subsequent median lengthscale.

GP with centroid covariates is the commonly-used approach (Bhatt et al. (2017); Mateo-Sanchis et al. (2019); Martinez-Ferrer et al. (2020)) and our results suggest that there are gains in both predictive performance and reduction in uncertainty when using aggregated output methods.

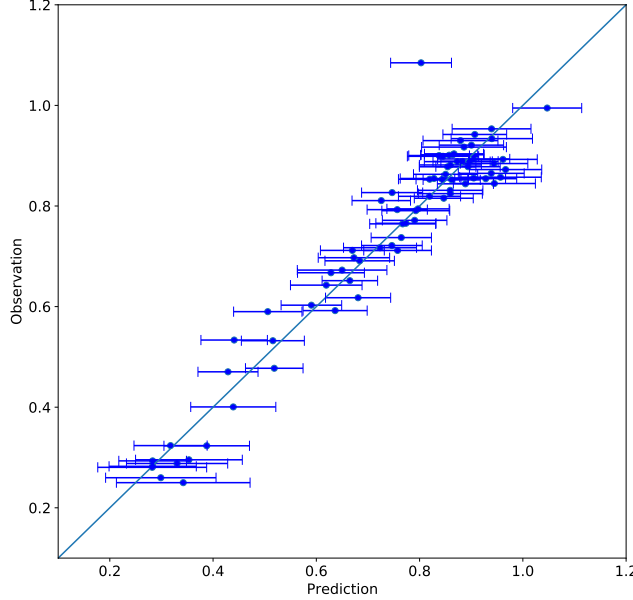


Figure 3: Prediction versus Observed Outputs with 95% posterior credible intervals on a test set of 20% of the points. 86.7% and 65.3% of the observations lie in the 95% and 80% credible intervals respectively.

Method	Covariates	RMSE	MAPE	Runtime (s)
LR	Centroid VOD + EVI	0.321 \pm 0.0446	0.411 \pm 0.0589	0.0457 \pm 0.00521
GP	Centroid VOD + EVI + space	0.0766 \pm 0.00782	0.0891 \pm 0.0113	1.26 \pm 0.0937
LRe	Stacked VOD + EVI	0.0752 \pm 0.00457	0.0846 \pm 0.00732	364 \pm 1.14
LRe	Stacked VOD + EVI + space	0.0726 \pm 0.00478	0.0798 \pm 0.00695	598 \pm 2.81
KRRe	Stacked VOD + EVI	0.0792 \pm 0.00514	0.0888 \pm 0.00828	1140 \pm 5.46
KRRe	Stacked VOD + EVI + space	0.0726 \pm 0.00554	0.0806 \pm 0.00826	1750 \pm 14.9
VBAgg	Stacked VOD + EVI	0.0758 \pm 0.00411	0.0850 \pm 0.00647	288 \pm 1.14
MVBAgg	Stacked VOD + EVI + space	0.0722 \pm 0.00454	0.0763 \pm 0.00619	478 \pm 0.485

Table 1: Cross-validated predictive and average run-time performance of the models on the crop yield data. We also report the standard error over 5-fold cross-validation of the RMSE and MAPE, as indicated as se-RMSE and se-MAPE respectively, and well as the standard error over the run-time.

LRe, the existing benchmark, requires hyperparameter tuning via cross-validation over a grid of configurations without the median heuristic. We also find that with our computational hardware, a full inference with VBAgg and MVBAgg is

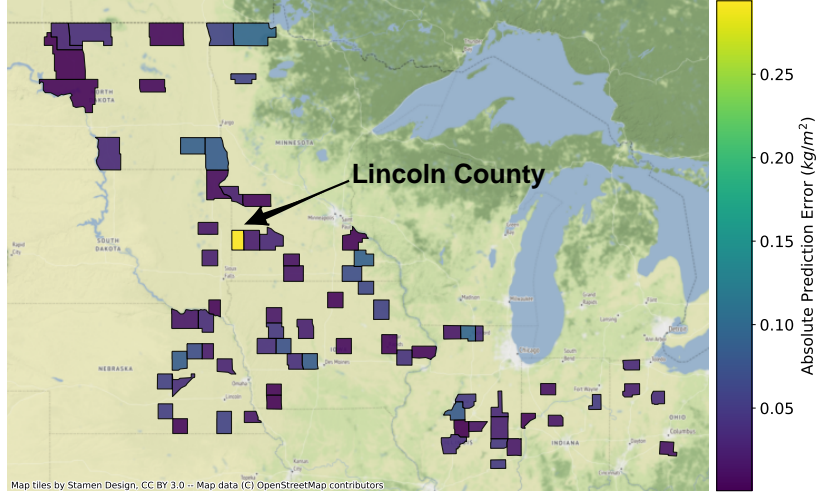


Figure 4: Absolute prediction error (kg/m^2) of MVBAgg on 75 counties that were held out as test set.

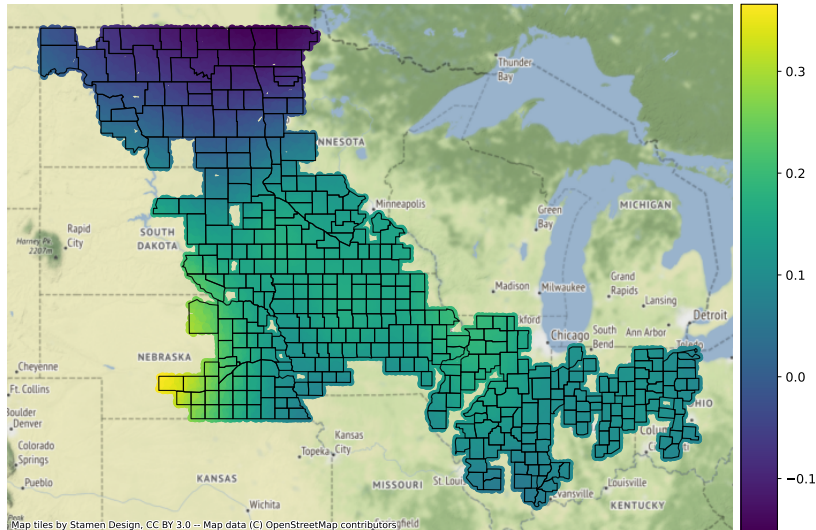


Figure 5: The spatial effects component of MVBAgg at the individual level after using the whole dataset for training.

faster than (See Table 1) fitting LRe or KRRe on a single set of hyperparameters, which confirms that our method is indeed more scalable.

As shown in Figure 4 of the prediction on 75 counties held out as test set, our model is unable predict well on Lincoln County, Minnesota which is an outlier as

can be seen in Figure 2. However, in Figure 3, we can see that most of the 95% posterior credible intervals for the test points contain the true crop yield. Finally, by looking at the posterior mean of the spatial component at the pixel-level in Figure 5, it is also interesting to see that we are able to uncover the additional spatial heterogeneity: for example, regions in Nebraska exhibit within-county variability as seen via the colour gradient within each county. This type of disaggregated information could be useful for agricultural policy makers to study where to impose interventions to improve productivity.

5 Conclusion

We developed a framework for spatial regression of aggregated outputs on multi-resolution covariates. Using Gaussian processes, we derived a multi-resolution version of VBAgg (Law et al. (2018a)), giving at least as good performance on a real world crop yield dataset as existing multi-resolution crop yield prediction models. In addition, our model is capable of performing inference on its model hyperparameters at scale and in a data-driven manner due to the variational formulation and the ability for GPU-acceleration, whereas kernel ridge regression requires tuning via cross-validation or the median-heuristic. We were also able to reconstruct the underlying fine-grained spatial effects by looking at the spatial component of MVBAgg and prediction uncertainty and we believe that this information would be particularly useful for organisations making policy interventions. We hope that this model could be useful for agriculture domain-experts who have access to other interesting crop yield datasets.

For future work, it would be interesting to consider our model for other problems such as disease mapping, as attempted previously by Law et al. (2018a) with VBAgg and Lucas et al. (2020). For improved performance with fewer observations of covariates in each county, it may be interesting to use control variates to give estimators with lower variance for the required integrals (Hammersley and Handscomb (1964)). Our model also makes the assumption that data for different resolutions are not dependent on each other, which may not be the case, and it would be useful to explore methods that can account for dependence without data up-sampling or down-sampling. It also may be of interest to explore alternative stochastic process priors for the underlying function other than GPs. Lastly, while our modelling approach is flexible for aggregation spatially, the dimensionality of the covariate space at each spatial location may be high and so it may be useful to consider learning low-dimensional projections within the model (Guhaniyogi and Dunson (2016); Delbridge et al. (2020)).

6 Acknowledgements

The authors would like to thank Hitesh Kumar and Jean-François Ton for useful feedback on a previous draft of the paper. HZ, AH were supported by the EPSRC Centre for Doctoral Training in Modern Statistics and Statistical

Machine Learning (EP/S023151/1) and the Department of Mathematics of Imperial College London. HZ was supported by Cervest Limited. AH was supported by the Bill and Melinda Gates Foundation. DS was supported in part by the Alan Turing Institute. SF was supported by the EPSRC (EP/V002910/1). We would also like to thank Andy Thomas for his endless support with using the NVIDIA4 GPU Compute Server. Many thanks to Gustau Camps-Valls and Anna Mateo-Sanchis for sharing the data used for their work.

References

Jose E Adsuara, Adrián Pérez-Suay, Jordi Muñoz-Marí, Anna Mateo-Sanchis, Maria Piles, and Gustau Camps-Valls. 2019. Nonlinear distribution regression for remote sensing applications. *IEEE Transactions on Geoscience and Remote Sensing* 57, 12 (2019), 10025–10035.

Samir Bhatt, Ewan Cameron, Seth R Flaxman, Daniel J Weiss, David L Smith, and Peter W Gething. 2017. Improved prediction accuracy for disease risk mapping using Gaussian process stacked generalization. *Journal of The Royal Society Interface* 14, 134 (2017), 20170520.

Douglas K. Bolton and Mark A. Friedl. 2013. Forecasting crop yield using remotely sensed vegetation indices and crop phenology metrics. *Agricultural and Forest Meteorology* 173 (May 2013), 74–84. <https://doi.org/10.1016/j.agrformet.2013.01.007>

Marshall Burke, Anne Driscoll, David B. Lobell, and Stefano Ermon. 2021. Using satellite imagery to understand and promote sustainable development. *Science* 371, 6535 (March 2021), eabe8628. <https://doi.org/10.1126/science.abe8628>

Alexander G De G. Matthews, Mark Van Der Wilk, Tom Nickson, Keisuke Fujii, Alexis Boukouvalas, Pablo León-Villagrá, Zoubin Ghahramani, and James Hensman. 2017. GPflow: A Gaussian process library using TensorFlow. *The Journal of Machine Learning Research* 18, 1 (2017), 1299–1304. Publisher: JMLR.org.

Ian Delbridge, David Bindel, and Andrew Gordon Wilson. 2020. Randomly projected additive Gaussian processes for regression. In *International Conference on Machine Learning*. PMLR, 2453–2463.

Kamel Didan. 2015. *MOD13Q1 MODIS/Terra Vegetation Indices 16-Day L3 Global 250m SIN Grid V006*. NASA EOSDIS Land Processes DAAC. <https://doi.org/10.5067/MODIS/MOD13Q1.006>

Dara Entekhabi, Eni G Njoku, Peggy E O'Neill, Kent H Kellogg, Wade T Crow, Wendy N Edelstein, Jared K Entin, Shawn D Goodman, Thomas J Jackson, Joel Johnson, and others. 2010. The soil moisture active passive (SMAP) mission. *Proc. IEEE* 98, 5 (2010), 704–716. Publisher: IEEE.

Seth Flaxman, Michael Chirico, Pau Pereira, and Charles Loeffler. 2019. Scalable high-resolution forecasting of sparse spatiotemporal events with kernel methods: A winning solution to the NIJ “Real-Time Crime Forecasting Challenge”. *The Annals of Applied Statistics* 13, 4 (2019), 2564–2585. <https://doi.org/10.1214/19-AOAS1284>

M Friedl and D Sulla-Menashe. 2015. MCD12C1 MODIS/Terra+ Aqua Land Cover Type Yearly L3 Global 0.05 Deg CMG V006 [Data set]. *NASA EOSDIS Land Processes DAAC* (2015).

Damien Garreau, Wittawat Jitkrittum, and Motonobu Kanagawa. 2018. Large sample analysis of the median heuristic. *arXiv:1707.07269 [math, stat]* (Oct. 2018). <http://arxiv.org/abs/1707.07269> arXiv: 1707.07269.

Alan E. Gelfand (Ed.). 2010. *Handbook of spatial statistics*. CRC Press, Boca Raton. OCLC: ocn176924834.

Rajarshi Guhaniyogi and David B Dunson. 2016. Compressed Gaussian process for manifold regression. *The Journal of Machine Learning Research* 17, 1 (2016), 2472–2497. Publisher: JMLR. org.

Oliver Hamelinck, Theodoros Damoulas, Kangrui Wang, and Mark Girolami. 2019. Multi-resolution Multi-task Gaussian Processes. In *Advances in Neural Information Processing Systems*, H. Wallach, H. Larochelle, A. Beygelzimer, F. d\textquotesingle Alché-Buc, E. Fox, and R. Garnett (Eds.), Vol. 32. Curran Associates, Inc. <https://proceedings.neurips.cc/paper/2019/file/0118a063b4aae95277f0bc1752c75abf-Paper.pdf>

John Michael Hammersley and David Christopher Handscomb. 1964. *Monte Carlo Methods*. Methuen. Google-Books-ID: Kk4OAAAAQAAJ.

Charles R. Harris, K. Jarrod Millman, Stéfan J. van der Walt, Ralf Gommers, Pauli Virtanen, David Cournapeau, Eric Wieser, Julian Taylor, Sebastian Berg, Nathaniel J. Smith, Robert Kern, Matti Picus, Stephan Hoyer, Marten H. van Kerkwijk, Matthew Brett, Allan Haldane, Jaime Fernández del Río, Mark Wiebe, Pearu Peterson, Pierre Gérard-Marchant, Kevin Sheppard, Tyler Reddy, Warren Weckesser, Hameer Abbasi, Christoph Gohlke, and Travis E. Oliphant. 2020. Array programming with NumPy. *Nature* 585, 7825 (Sept. 2020), 357–362. <https://doi.org/10.1038/s41586-020-2649-2> Publisher: Springer Science and Business Media LLC.

Manuel Haussmann, Fred A. Hamprecht, and Melih Kandemir. 2017. Variational Bayesian Multiple Instance Learning with Gaussian Processes. In *2017 IEEE Conference on Computer Vision and Pattern Recognition (CVPR)*. IEEE, Honolulu, HI, 810–819. <https://doi.org/10.1109/CVPR.2017.93>

James Hensman, Nicolò Fusi, and Neil D. Lawrence. 2013. Gaussian Processes for Big Data. In *Proceedings of the Twenty-Ninth Conference on Uncertainty in Artificial Intelligence (UAI'13)*. AUAI Press, Arlington, Virginia, USA, 282–290. event-place: Bellevue, WA.

James Hensman, Alexander Matthews, and Zoubin Ghahramani. 2015a. Scalable variational Gaussian process classification. In *Artificial Intelligence and Statistics*. PMLR, 351–360.

James Hensman, Alexander G de G Matthews, Maurizio Filippone, and Zoubin Ghahramani. 2015b. MCMC for variationally sparse Gaussian processes. *arXiv preprint arXiv:1506.04000* (2015).

Maximilian Ilse, Jakub Tomczak, and Max Welling. 2018. Attention-based deep multiple instance learning. In *International conference on machine learning*. PMLR, 2127–2136.

Motonobu Kanagawa, Philipp Hennig, Dino Sejdinovic, and Bharath K. Sriperumbudur. 2018. Gaussian Processes and Kernel Methods: A Review on Connections and Equivalences. *arXiv:1807.02582 [cs, stat]* (July 2018). <http://arxiv.org/abs/1807.02582> arXiv: 1807.02582.

Minyoung Kim and Fernando De la Torre. 2010. Gaussian processes multiple instance learning. In *ICML*.

Alexandra G. Konings, Maria Piles, Narendra Das, and Dara Entekhabi. 2017. L-band vegetation optical depth and effective scattering albedo estimation from SMAP. *Remote Sensing of Environment* 198 (Sept. 2017), 460–470. <https://doi.org/10.1016/j.rse.2017.06.037>

Kentaro Kuwata and Ryosuke Shibasaki. 2015. Estimating crop yields with deep learning and remotely sensed data. In *2015 IEEE International Geoscience and Remote Sensing Symposium (IGARSS)*. IEEE, 858–861.

Ho Chung Law, Dino Sejdinovic, Ewan Cameron, Tim Lucas, Seth Flaxman, Katherine Battle, and Kenji Fukumizu. 2018a. Variational learning on aggregate outputs with Gaussian processes. In *Advances in Neural Information Processing Systems*. 6081–6091.

Ho Chung Leon Law, Dougal Sutherland, Dino Sejdinovic, and Seth Flaxman. 2018b. Bayesian approaches to distribution regression. In *International Conference on Artificial Intelligence and Statistics*. PMLR, 1167–1176.

Maud Lemercier, Christopher Salvi, Theodoros Damoulas, Edwin Bonilla, and Terry Lyons. 2021. Distribution Regression for Sequential Data. In *Proceedings of The 24th International Conference on Artificial Intelligence and Statistics (Proceedings of Machine Learning Research, Vol. 130)*, Arindam Banerjee and Kenji Fukumizu (Eds.). PMLR, 3754–3762. <http://proceedings.mlr.press/v130/lemercier21a.html>

David B. Lobell, David Thau, Christopher Seifert, Eric Engle, and Bertis Little. 2015. A scalable satellite-based crop yield mapper. *Remote Sensing of Environment* 164 (July 2015), 324–333. <https://doi.org/10.1016/j.rse.2015.04.021>

Tim C.D. Lucas, Anita K. Nandi, Suzanne H. Keddie, Elisabeth G. Chestnutt, Rosalind E. Howes, Susan F. Rumisha, Rohan Arambepola, Amelia Bertozzi-Villa, Andre Python, Tasmin L. Symons, Justin J. Millar, Punam Amratia, Penelope Hancock, Katherine E. Battle, Ewan Cameron, Peter W. Gething, and Daniel J. Weiss. 2020. Improving disaggregation models of malaria incidence by ensembling non-linear models of prevalence. *Spatial and Spatio-temporal Epidemiology* (July 2020), 100357. <https://doi.org/10.1016/j.sste.2020.100357>

Oded Maron and Tomás Lozano-Pérez. 1998. A framework for multiple-instance learning. In *Advances in neural information processing systems*. 570–576.

Laura Martinez-Ferrer, Maria Piles, and Gustau Camps-Valls. 2020. Crop Yield Estimation and Interpretability With Gaussian Processes. *IEEE Geoscience and Remote Sensing Letters* (2020), 1–5. <https://doi.org/10.1109/LGRS.2020.3016140>

Anna Mateo-Sanchis, Maria Piles, Jordi Muñoz-Marí, Jose E. Adsuara, Adrián Pérez-Suay, and Gustau Camps-Valls. 2019. Synergistic integration of optical and microwave satellite data for crop yield estimation. *Remote Sensing of Environment* 234 (Dec. 2019), 111460. <https://doi.org/10.1016/j.rse.2019.111460>

Krikamol Muandet, Kenji Fukumizu, Francesco Dinuzzo, and Bernhard Schölkopf. 2012. Learning from Distributions via Support Measure Machines. In *NIPS*. 10–18. <http://papers.nips.cc/paper/4825-learning-from-distributions-via-support-measure-machines>

Dino Oglic and Thomas Gärtner. 2017. Nyström Method with Kernel K-means++ Samples as Landmarks. In *Proceedings of the 34th International Conference on Machine Learning (Proceedings of Machine Learning Research, Vol. 70)*, Doina Precup and Yee Whye Teh (Eds.). PMLR, 2652–2660. <http://proceedings.mlr.press/v70/oglic17a.html>

Ali Rahimi and Benjamin Recht. 2008. Random features for large-scale kernel machines. In *Advances in neural information processing systems*. 1177–1184.

Carl Edward Rasmussen. 2003. Gaussian processes in machine learning. In *Summer School on Machine Learning*. Springer, 63–71.

H. Rue, A. Riebler, S. H. Sørbye, J. B. Illian, D. P. Simpson, and F. K. Lindgren. 2016. Bayesian computing with INLA: A review. *Annual Reviews of Statistics and Its Applications* 4 (2016), 395–421.

Anna Mateo Sanchis, Jose Adsuara, Maria Piles, Adrián Perez-Suay, Jordi Muñoz-Marí, and Gustau Camps-Valls. 2019. Multisensor distribution regression for crop yield estimation.. In *Geophysical Research Abstracts*, Vol. 21.

Jiaxin Shi, Michalis Titsias, and Andriy Mnih. 2020. Sparse orthogonal variational inference for gaussian processes. In *International Conference on Artificial Intelligence and Statistics*. PMLR, 1932–1942.

Zoltán Szabó, Bharath K Sriperumbudur, Barnabás Póczos, and Arthur Gretton. 2016. Learning theory for distribution regression. *The Journal of Machine Learning Research* 17, 1 (2016), 5272–5311. Publisher: JMLR. org.

Yusuke Tanaka, Toshiyuki Tanaka, Tomoharu Iwata, Takeshi Kurashima, Maya Okawa, Yasunori Akagi, and Hiroyuki Toda. 2019. Spatially aggregated Gaussian processes with multivariate areal outputs. In *Advances in Neural Information Processing Systems*. 3000–3010.

Daniel Thorns. 2018. *Distribution Regression for Crop Yield Prediction*. Master’s thesis. Department of Statistics, Oxford University, United Kingdom.

Michalis Titsias. 2009. Variational learning of inducing variables in sparse Gaussian processes. In *Artificial Intelligence and Statistics*. 567–574.

Jean-Francois Ton, Seth Flaxman, Dino Sejdinovic, and Samir Bhatt. 2018. Spatial mapping with Gaussian processes and nonstationary Fourier features. *Spatial Statistics* 28 (Dec. 2018), 59–78. <https://doi.org/10.1016/j.spasta.2018.02.002>

Qi Yang, Liangsheng Shi, and Lin Lin. 2019. Plot-scale rice grain yield estimation using UAV-based remotely sensed images via CNN with time-invariant deep features decomposition. In *IGARSS 2019 - 2019 IEEE International Geoscience and Remote Sensing Symposium*. IEEE, Yokohama, Japan, 7180–7183. <https://doi.org/10.1109/IGARSS.2019.8898061>

Jiaxuan You, Xiaocheng Li, Melvin Low, David Lobell, and Stefano Ermon. 2017. Deep gaussian process for crop yield prediction based on remote sensing data. In *Thirty-First AAAI Conference on Artificial Intelligence*.

Fariba Yousefi, Michael T Smith, and Mauricio Álvarez. 2019. Multi-task Learning for Aggregated Data using Gaussian Processes. In *Advances in Neural Information Processing Systems*, H. Wallach, H. Larochelle, A. Beygelzimer, F. d\textquotesingle Alché-Buc, E. Fox, and R. Garnett (Eds.), Vol. 32. Curran Associates, Inc. <https://proceedings.neurips.cc/paper/2019/file/64517d8435994992e682b3e4aa0a0661-Paper.pdf>

Cheng Zhang, Judith Butepage, Hedvig Kjellstrom, and Stephan Mandt. 2019. Advances in Variational Inference. *IEEE Transactions on Pattern Analysis and Machine Intelligence* 41, 8 (Aug. 2019), 2008–2026. <https://doi.org/10.1109/TPAMI.2018.2889774>

Yivan Zhang, Nontawat Charoenphakdee, Zhenguo Wu, and Masashi Sugiyama. 2020. Learning from Aggregate Observations. In *Advances in Neural Information Processing Systems*, H. Larochelle, M. Ranzato, R. Hadsell, M. F. Balcan, and H. Lin (Eds.), Vol. 33. Curran Associates,

Inc., 7993–8005. <https://proceedings.neurips.cc/paper/2020/file/5b0fa0e4c041548bb6289e15d865a696-Paper.pdf>